Energy, Mines and Resources Canada | Énergie, Mines et Ressources Canada

CANMET

Canada Centre for Mineral and Energy Technology | Centre canadien de la technologie des minéraux et de l'énergie

FATIGUE CRACK PROPAGATION IN WELDED PLATE T-JOINTS
INTERIM REPORT

O. VOSIKOVSKY and A.RIVARD
ENGINEERING SECTION

MAY 1984

[illegible] report
[illegible] rapport intérimaire
for distribution [illegible]
reporting [illegible]
represent [illegible]
the [illegible]
fo [illegible]
(CANMET) [illegible] de
[illegible] et de

ENERGY RESEARCH PROGRAM

34 pp

PHYSICAL METALLURGY RESEARCH LABORATORIES
REPORT: ERP/PMRL 84-30(TR)

MICROMEDIA
FEB 27 1985

PHYSICAL METALLURGY RESEARCH LABORATORIES
REPORT ERP/PMRL 84-30(TR)

FATIGUE CRACK PROPAGATION IN WELDED PLATE T-JOINTS
INTERIM REPORT

by

O. Vosikovsky and A. Rivard

ABSTRACT

The experimental techniques used for fatigue testing and monitoring of crack growth of welded plate T-joints 16 to 102 mm thick are reported. The results of the first eight tests on 28 and 52 mm thick joints are evaluated and prospects for using fracture mechanics for accurate prediction of crack propagation fatigue life are assessed.

RÉSUMÉ

Nous décrivons les techniques expérimentales utilisées pour les ersais de fatigue et l'évaluation de la croissance de fissures aux joints de soudure en T de tôles de 16 à 102 mm d'épaisseur. Nous analysons les résultats des huit premiers essais sur les joints de 28 et 52 mm et nous évaluons les perspectives d'utilisation de la mécanique de la rupture pour prédire de façon précise la durée de ire en fatigue-propagation.

1. Introduction

The development of methods for fatigue life assessment of welded joints in offshore structures has progressed considerably during last few years. The traditional design method based on S-N curves, particularly with application to welded tubular joints, has been refined and the effects of many parameters influencing fatigue life clarified by extensive research programs [1-2]. The effect of increasing plate thickness on reduction of fatigue life was incorporated in the new design rules [3-4].

An alternative method for fatigue life assessment, based on fatigue crack propagation and fracture mechanics has also made progress [5-7]. It has been established that the fatigue life of tubular joints is dominated by propagation of a sizeable crack [2-6]. For welded plate joints the crack remains small for a major part of its life and the crack initiation period may be more significant than the initiation period in tubular joints [2-7]. The fracture mechanics approach for assessment of fatique life of welded joints has been accepted as an alternative to the method based on S-N curves by the DnV rules for design of offshore structures [8].

The fracture mechanics approach offers several advantages over the traditional S-N design method:

1. If an initial defect is detected in a manufactured joint or during an in-service inspection, the residual fatigue life can be assessed.
2. The effect of aggressive environments on fatigue crack growth rate can be determined using relatively cheap laboratory tests. Basic data on the effects of sea water on fatigue crack growth rates in structural steels are available [9-10].
3. The effect of thickness on fatigue life is predictable by fracture mechanics [5-7].

Wide use of fracture mechanics has been hindered so far by lack of accurate solutions for stress intensity factors in two dimensional surface cracks in welded joints, and by difficulties in accurately sizing fatigue cracks by NDT techniques.

The CANMET research project "Materials for Offshore Structures" initially focuses on fatigue behaviour of welded T-joints loaded through the attachment plate under constant amplitude. To evaluate the effect of thickness, joints 16, 28, 52, 76 and 102 mm thick are being tested. The development of the first cracks, and their subsequent coalescence and growth is

accurately monitored using AC potential drop, and beach marking techniques. Simultaneously the stress intensity factors for surface cracks of weld toes are determined, using finite element analyses, for the joint geometries used in the experimental program [11]. The fatigue lives determined from fracture mechanics analysis for an appropriate variation in crack shape will be compared with experimental lives. Thus an evaluation of the accuracy of fracture mechanics predictions, including size effects, will be possible.

In this interim report the development of techniques for T-joint testing and crack growth monitoring are described. The results from the first eight tests with plate thicknesses of 28 and 52 mm are reported.

2. Material and test joints

The chemical composition and mechanical properties of steel plates (16, 28, 52, 76 and 102 mm thick) used in the manufacture of T-joints are listed in Table 1. The plates 16 and 102 mm thick manufactured to CSA G40.21 Grade 350 WT are control rolled. The remaining plates were manufactured to Lloyd's LT60 specification, and are normalized. The minimum Charpy-V notch toughness for all plates is 41 J at -60°C.

Figure 1 shows the design of the welded T-joints. Welding was carried out in accordance with the requirements set by United Kingdom Offshore Steels Research Project, Phase II. All specimens were welded manually in the vertical-up position using E7018 electrodes of 2.5 and 4 mm diameter. Plates with 52 mm and higher thicknesses were pre-heated to a minimum temperature of 100°C. All specimens with the exception of the first six 28 mm thick joints had a controlled weld profile achieved by applying the buttering pass at the weld toe as the first run. For the six specimens with uncontrolled weld profiles, the bead forming the weld toe was deposited as the last pass. In addition, the first two 28 mm thick specimens were restrained during welding in an attempt to prevent distortion.

The weld-toe radius r and angle θ were measured on the sectioned plaster casts of weld profiles. Ten measurements for each specimen were made on enlarged photographs of cross-sections of the cast.

3. Experimental Techniques

3.1 Testing conditions

The T-joints were tested by 3-point bending in laboratory air under sinusoidal cyclic loads. The load ratio $R = \frac{P_{min}}{P_{max}}$ was kept constant at 0.05 and the cyclic frequency varied between 5 and 10 Hz. The loads were selected to produce a nominal stress range at the weld toe of either 100 or 150 MPa.

Loads were applied through pin connections to the attachment plate by a vertical hydraulic actuator (Fig. 2). To achieve proper alignment of warped specimens the position and tilt of reaction beams were made adjustable by two set screws (see Fig. 2).

The alignment of each specimen was checked by two strain gauges attached to the centre of the base plate 20 mm from the weld toes. One specimen of each thickness was instrumented with a strip gauge to measure the effect of thickness on stress distribution near the weld toe. The strain measurements were done at incrementally increased loads after application of about 200 load cycles.

3.2 Crack growth monitoring

The crack depth a, during the fatigue test was measured using a multiprobe AC potential technique [12]. Initially 10 probes (each consisting of one active pair and one reference pair) spaced 20 mm apart were used. Later, the probe arrangement was modified such that 18 active probes spaced 10 mm apart with two reference probes (1 reference for each 9 active pairs on the right and left half length of the weld) were used.

Closer spacing of the probes was adopted to ensure that the first initiating crack was detected and monitored. The "denser" probe arrangement is shown in Fig. 3.

Each active or reference pair consisted of two spot-welded low carbon steel wires at a distance of ~10 mm. The potential signal was fed into the "Unit Inspection Crack Micro Gauge" through the 20 channel low voltage switching unit (Fig. 2). An AC current was introduced into the attachment and base plates at a distance of 210 mm from the weld. The amplified DC output of the crack gauge was linked to a computer and the potential distribution along the weld-toe length was scanned periodically to determine the increments in crack depth growth during the test. To ensure that the cracks initiated at the instrumented weld the weld toe on the opposite side of attachment plate was ground and lightly peened.

The second method, used for determination of crack shape and calibration of AC potential measurements, was to introduce four or five beach-marks during each test. Ink staining was used to identify the first beach mark. The remaining beach marks were created by decreasing the load amplitude by half and doubling the frequency for an appropriate number of cycles (10 to 120 k cycles - depending on crack depth and stress range). An example of beach marks on a 28 mm thick joint is shown in Fig. 4. The locations of the AC potential probes spaced 20 mm apart can be seen.

For a uniform current field distribution and a straight fronted crack, the crack depth can be calculated from the following equation [12]:

$$a = \frac{\Delta}{2}\left(\frac{V_a}{V_o} - 1\right) \tag{1}$$

where Δ is the probe length, V_a is the potential across the crack and V_o is the reference potential next to the crack. For the spot welded probes at the toe of a weld the inital ratio of $\frac{V_{(a=o)}}{V_o}$ did not always equal one and equation (1) was modified to:

$$a = A\left[\left(\frac{V}{V_o}\right)_a - \left(\frac{V}{V_o}\right)_o\right], \tag{2}$$

where $\left(\frac{V}{V_o}\right)_o$ is the initial ratio of active and reference potentials (before a crack initiated) and $\left(\frac{V}{V_o}\right)_a$ is the ratio of the potentials for crack depth a. A is a calibration constant determined from crack depth under the individual probe, indicated by beach marks. An example of a typical set of calibration curves is given in Fig. 5. It can be seen that equation (2) holds only for cracks up to 8 to 10 mm deep, and that A varies widely for individual probes. These deviations in shape of actual calibration curves from the theoretical calibration curve (dashed line with slope A = 5) are apparently caused by irregular shape of cracks, non-uniformity of the current field and spurious potentials picked up by the leads. Changing the arrangement of current and potential leads has so far failed to produce a single calibration curve close to the theoretical one that could be applicable to all leads. As a result the individual empirical calibration curves had to be used for determination of crack depths. The accuracy of crack depth determination is estimated to be better than ± 1 mm.

4. Experimental results

4.1 Weld-toe geometry

The measurements of weld-toe geometry are summarized in Table 2. Both the angle and radius vary widely along the weld length. The mean values of radius are about the same for improved and unimproved weld profiles. However, the mean weld-toe angle for an unimproved profile is considerably higher, 60° compared with 37.5° for an improved profile.

4.2 Stresses of the weld toe

The nominal stress ranges calculated from simple beam theory at the weld toe, and weld-toe stress ranges - linearly extrapolated from strain gauge measurements on both sides of the attachment plate, are listed in Table 3, together with total and crack initiation fatigue lives. The stress ranges measured by strain gauge are on average 4% lower than the nominal ones. The differences between the stress range measurements on each side of the attachment plate are smaller than 8%, indicating reasonably good specimen alignment. In Fig. 6 the stress distribution near the weld toe measured by strip gauges on one specimen of each thickness is compared with the stress distribution determined by finite element (FE) analysis [11]. The measured stresses reflect the effect of thickness, however, when compared to FE calculations they are almost 10% lower.

4.3 Fatigue life

A crack depth of 0.5 mm was taken as the initiation value. Similarly the total life was defined by a maximum crack depth equal to one half the specimen thickness. Tests were carried out until the crack depth reached about two thirds of the thickness. However, when the crack depth exceeded half thickness the growth rate was so high that additional life was less than 1% of the total. As a result $a = 0.5\ t$ was chosen as an unambiguous definition of the total fatigue life.

The initiation and total fatigue lives listed in Table 3 are compared, in Fig. 7, with the mean life curve for 38 mm thick cruciform joints tested at $R = 0$ and -1 from [4]. The fraction of the total life required to initiate a 0.5 mm deep crack, listed in Table 3, varied from 22 to 31%.

4.4 Propagation of fatigue cracks

After completion of fatigue tests, the specimens were fractured, the crack depths under the probes indicated by the beach marks were measured, and calibration curves (Fig. 5) were drawn. The first beach mark produced by ink staining gave an indication of the number, distribution, and shape of the initial cracks (Fig. 4). About fifteen cracks per specimen were detected in the 28 mm thick plates with unimproved weld profile compared with about ten in 52 mm thick specimens with improved weld profiles. The subsequent beach marks provided information on change of crack shape, governed by coalescence of single cracks. The development of crack shape is shown in Figs. 8a & b where aspect ratios $\frac{a}{c}$ (a - maximum crack depth , 2c crack length on the surface) are plotted vs depth for 28 and 52 mm thick joints. In both cases the first cracks initiate with an aspect ratio close to one. As the first cracks coalesce the aspect ratio drops steeply. When the crack depth reaches either ~4 mm (for 28 mm joints) or ~6 mm (for 52 mm joints) the aspect ratio levels off at ~0.15. The surface cracks turn into through cracks at depths ranging from 9 to 14 mm. The first cracks always initiated in the central length of weld toe, at least 20 mm from the edges.

For each test the potentials from two probes, closest to the deepest point on the two first initiating cracks, were converted into crack depths and the resulting a vs N curves are shown in Figs. 9-14. With probe spacings of 20 mm the first crack sometimes initiated in between the probes, or the probe was located too far off centre of the deepest crack. This was the case in the 52 mm thick joint, No. 1, where the first two deepest cracks were located exactly in between probes. In the 28 mm thick joint No. 6 the probes were located off centre of the two deepest cracks. As a result the measured crack initiation lives do not represent the deepest crack and are too long. The problem was rectified by reduction of the probe spacing from 20 to 10 mm.

The crack growth curves for the first initiating crack in Figs. 9-14 have (with the exception of Figs. 12 & 13 where the first crack was missed) a common feature: the crack depth between 1 and ~8 mm corresponding to 50 - 60% of the total fatigue life varies almost linearly with the number of cycles.

The displacement range variations monitored as the actuator displacements $\Delta\ell$ are also shown in Figs. 9-14. It can be seen that $\Delta\ell$ remains constant until the crack depth reaches one quarter to one third of plate thickness. An abrupt increase in displacement occurs when the surface crack becomes a "through the width" crack. If the deepest crack initiated off centre

from the weld length, resulting in a slant crack (spec. No. 3,5 t = 28 - Figs. 9-11) the increase in $\Delta\ell$ was gradual until the crack broke through the plate edge on both sides. The abrupt increase in $\Delta\ell$ is accompanied by sharp increase in crack growth rate and terminates the useful life of the joint.

5. Discussion of Results and Conclusions

The main intention of this interim report is to describe the development of experimental techniques used for evaluation of fracture mechanics predictions of fatigue life, and size effects in plate welded T-joints. About one quarter of the planned tests in air have been completed to date. Thus only limited discussion of some emerging trends is warranted.

Design of welded T-joints with load-carrying welds, loaded in three-point bending through the attachment plate, was chosen to simulate loading in tubular joints. Initial tests show that good joint alignment can be achieved in the specially designed loading frames.

The measured total fatigue lives are comparable to those measured on cruciform specimens reported in [4], Fig. 7. The exceptions are the first two joints welded under restrained conditions. The joint tested in a stress range of 150 MPa failed from the ground weld toe making the life of the as-welded side of the weld more than three times longer than the mean life of cruciform joints. The joint tested at $\Delta\sigma$ = 200 MPa had a life almost three times longer than the cruciform joints.

Apparently, the spring-back of the base plate after removal of the restraint created compressive residual stresses in the weld toe. These residual stresses produced increased fatigue life comparable to those obtained by peening.

Accurate monitoring of fatigue crack growth from the first initiating crack to end of life was attempted. The beach marks provided information on location of the first initiating cracks, change of crack shape resulting from coalescence and growth, and a means of calibrating the AC potential apparatus. The beach-mark measurements indicate that the number of initiating cracks depends on weld-toe geometry. In specimens with unimproved weld profile, and with steeper weld-toe angle (Table 2), a greater number of cracks initiated in the same length of weld. The change in shape of growing cracks is dominated by crack coalescence. As can be seen from Figs. 8(a), & (b) the drops in the

aspect ratio with crack depth in specimens with unimproved weld profiles was steeper than in specimens with improved weld profiles. A comparison of lives of 28 and 52 mm thick joints shows correct size effect [3], however, the comparison may not be valid since the two sets of specimens had different weld-toe geometries.

The AC technique showed satisfactory stability during long tests. However, the conversion of measured potentials into crack length was cumbersome since every specimen and potential probe produced a different calibration curve (Fig. 5). Only the initial parts of the calibration curves for shallow cracks are linear. Attempts at modification of current and potential lead arrangements to simplify calibration are still under way. The probe spacing of 20 mm used initially proved to be inadequate since in two specimens the first initiating cracks were missed. The increased number of probes with 10 mm spacing should correct this problem.

For the specimens where the first crack was detected by a correctly located probe (Figs. 9, 10, 11, 14) the initiation life for a 0.5 mm deep crack was close to 25% of the total life. During the subsequent 60% of life the crack depth extended to 8 ~ 11 mm and was still contained within the specimen width as a surface crack. During this life period the crack-growth curves are almost linear, similar to the crack growth behaviour of tubular joints [6].

An initial attempt to assess the capability of fracture mechanics to predict fatigue life has been made for 28 mm thick joints. The fatigue crack growth rates were determined from slopes of crack-growth curves in Fig. 9-12. The corresponding stress intensity ranges for semielliptical cracks were obtained from finite element (FE) solutions for this specimen geometry, from reference [11]. Variation of crack shape with depth was assumed to be given by a fitted mean curve in points measured from beach marks in Fig. 8a. The determined crack growth rates for cracks 0.5 to 4.5 mm deep are plotted vs stress intensity ranges in Fig. 15, together with fatigue crack growth rates for a variety of stress ratios, measured on standard specimens made of similar offshore steel [9]. The lower set of the growth rate data, corresponding to a stress range of 100 MPa, indicates a curve which would cross over the data from ref. [9]. This behaviour can be expected since the welded joints contain high tensile residual stress close to the weld toe, changing to compressive stress as the distance from the surface increases. As a result the tip of a

growing crack initially experiences a high positive R, which changes rapidly to negative values as the crack grows deeper. The growth rates close to the threshold, as can be seen from Fig. 15, are strongly influenced by the stress ratio, and its effect is reflected in growth rates measured on welded T-joints. The upper set of growth rate data corresponding to the stress range of 150 MPa falls well above the threshold range. At higher ΔK the effect of stress ratio is much less significant, and as a result the "cross-over" of the indicated growth rate curve for a welded specimen is less pronounced.

The agreement of measured growth rates in standard and welded specimens provides encouragement that a numerical integration procedure for calculation of crack-propagation life can be developed. However, for accurate prediction of long lives, associated with shallow initial cracks and low stress ranges, residual stress distribution in the weld may have to be accounted for.

References

1. European Offshore Steel Research Seminar, Cambridge, November 1978.

2. International Conference on Steel in Marine Structures, Paris, October 1981.

3. Offshore Installations: Guidance on design and construction - proposed new fatigue design rules for steel welded joints in offshore structures, U.K. Department of Energy, 1981.

4. Background to proposed new fatigue design rules for steel welded joints in offshore structures, U.K. Department of Energy, 1981.

5. T.R. Guerney "The influence of thickness on the fatigue strength of welded joints", Boss Conference, London, Paper 41, (August 1979).

6. F.D. Dover and S. Dharmavason "Fatigue fracture mechanics analysis of T and Y joints", OTC Conference, Houston, Paper 4404, (May 1982).

7. S. Berge "Effect of plate thickness in fatigue of cruciform welded joints", Report MK/R67, Department of Marine Technology - the Norwegian Institute of Technology, University of Trondheim, (March 1983).

8. Rules for the Design Construction and Inspection of Offshore Structures, Appendix C, Det norske Veritas, 1977.

9. T.W. Thorpe, P.M. Scott, A. Rance and D. Silvester "Final report for the U.K. offshore steel research project corrosion-fatigue of B.S. 4360:50D structural steel in seawater". AERE report R 10679, AERE Horwell, (Nov. 1982).

10. O. Vosikovsky, W.R. Neill, D.A. Carlyle and A. Rivard "The effect of seawater temperature on corrosion fatigue crack growth in structural steels", CANMET Report ERP/PMRL 83-27(OP-J), (April 1983).

11. R. Bell and J. Kirkhope "Determination of stress intensity factors for weld toe defects", CANMET Contract Report DSS File No. 14SV.23440-2-9083, (April 1983).

12. F.D.W. Charlesworth and W.D. Dover "Some aspects of crack detection and sizing using AC field measurements", Advances in crack length measurement, Editor C.J. Beevers, 253-276, EMAS 1982.

Table 1. Chemical composition and mechanical properties

Chemical composition:					
	Plate thickness mm				
	16	28	52	76	102
C	0.07		0.12		0.13
Mn	1.40		1.39		1.43
Si	0.29		0.28		0.23
S	0.005		0.011		0.003
P	0.004		0.017		0.013
Al	0.045		0.027		0.015
Ni	0.25		0.15		0.24
Cr	0.25		0.17		none
Mo	none		0.01 or less		none
Cu	none		0.15		none
Ti	0.012		none		0.006
V	0.075		0.053		0.06
Nb	0.022		0.041		0.02
N	0.01		-		0.01
Mechanical properties:					
Yield strength (MPa)	421	405	390	370	350
UTS (MPa)	509	513	517	505	502
Elongation (%)	53	29	32	31	38

Table 2. Weld toe geometry of welded joints

Plate thickness mm	Spec. No.	Leg length (mm)	Weld toe angle θ Deg.	Mean $\bar{\theta}$ Deg.	Weld toe radius r mm	Mean $\bar{r}$ mm	Comment
28	3	18/22	38 ÷ 79	60	0.5 ÷ 5.1	1.4	Unimproved
	4	"	"	"	"	"	weld
	5	"	"	"	"	"	profile
	6	"	"	"	"	"	
52	1	30 ÷ 32	33 ÷ 57	38	0.2 ÷ 3.2	1.6	Improved
	2	"	28 ÷ 48	37	0.3 ÷ 1.8	1.0	weld profile

Table 3. Stress ranges and fatigue lives of tested joints

Plate thickness mm	Spec. No.	Stress range at the weld toe			Fatigue life			
		Nominal	Measured by strain gauge		Initiation 0.5 mm crack Ni	Total N	Ni/N	
			Instrumented toe	Ground toe				
		MPa	MPa	MPa	kcycles	kcycles	%	
28	1	150	-	-	-	>1590	-	Unimproved weld profile, welded restrained
	2	200	-	-	-	580	-	
	3	150	147	152	160	595	27	Unimproved weld profile
	4	100	100	92	340	1410	24	
	5	100	95	96	430	1910	23	
	6	150	136	148	205	700	29	
52	1	100	97	94	380	1210	31	Improved weld profile
	2	150	142	138	80	370	22	

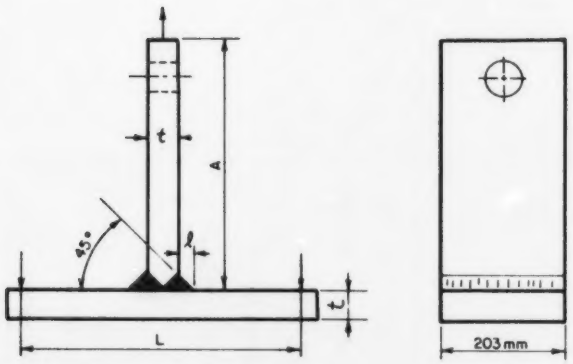

JOINT	t mm	l mm	L mm	A mm
A	16	8-12	300	406
B	28	14-18	442	406
C	52	26-30	442	406
D	78	38-42	584	457
E	102	52-56	726	457

Fig. 1. Dimensions of tested welded T-joints. (neg 10504)

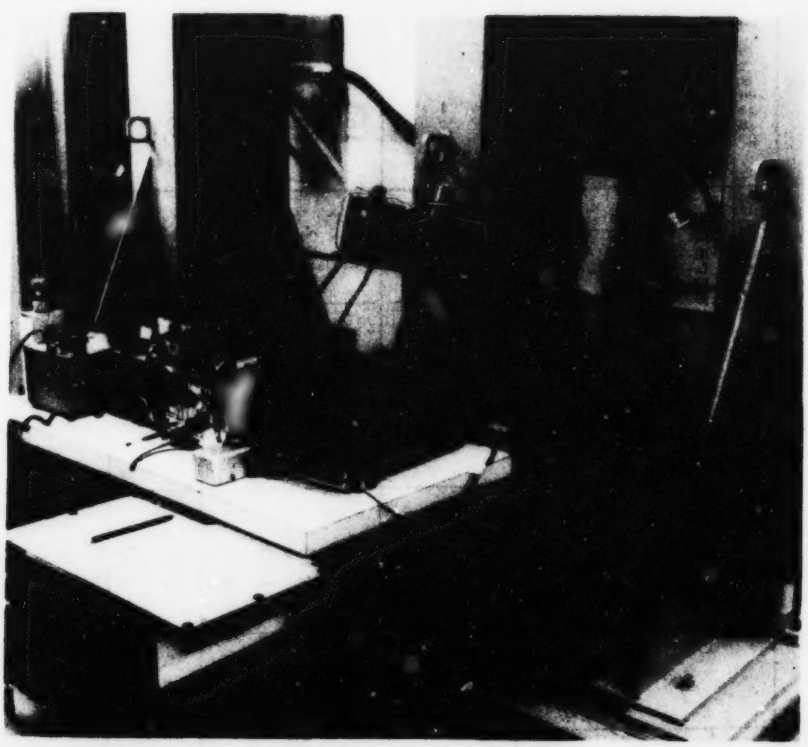

Fig. 2. The 52 mm T-joint in the test frame and instrumentation used for AC potential measurements. (neg 10393)

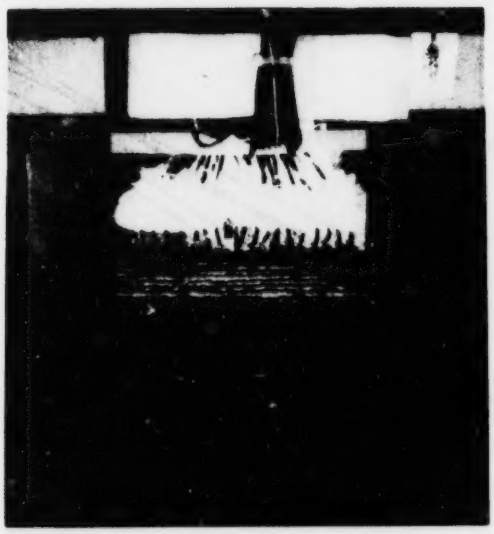

Fig. 3. Arrangement of AC potential probes on 52 mm thick T-joint, spec. No.2. (neg 10394)

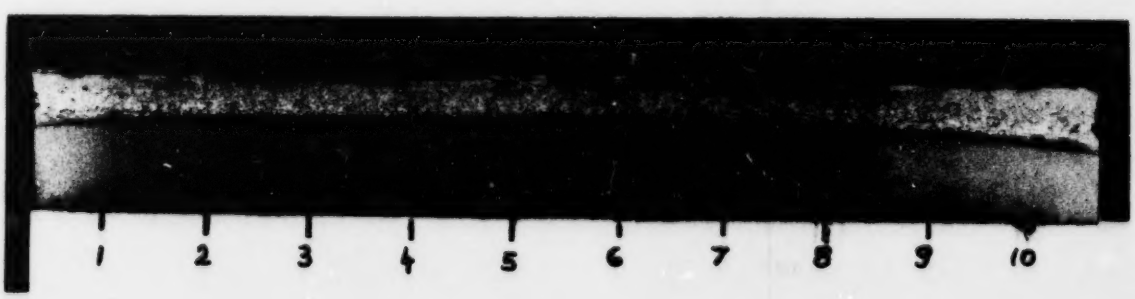

Fig. 4. Beach marks and locations of potential probes on fractured 28 mm thick T-joint, spec. No. 4. (neg 10068)

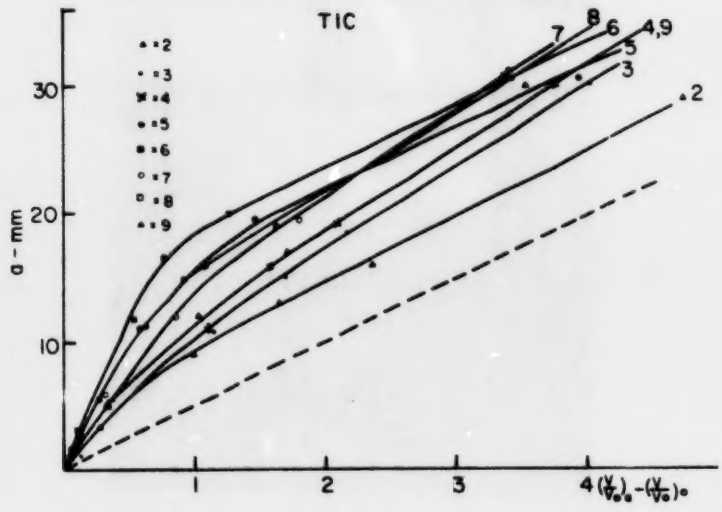

Fig. 5. Calibration curves for individual probes on 52 mm thick T-joint, spec. No.2. The dashed line is the theorotical calibration curve. (neg 10500)

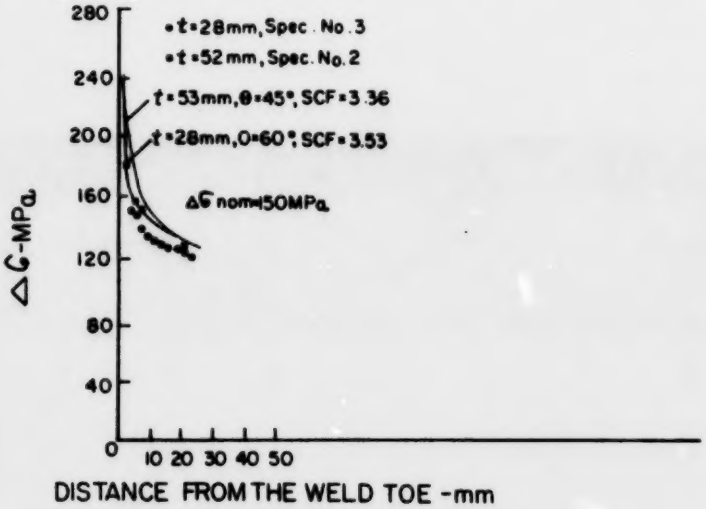

Fig. 6. Distribution of stresses near the weld toe measured by strip gauges (points), and determined from FE analysis (curves) for 28 mm, (No.3) and 52 mm (No.2) thick T-joints. (neg 10501)

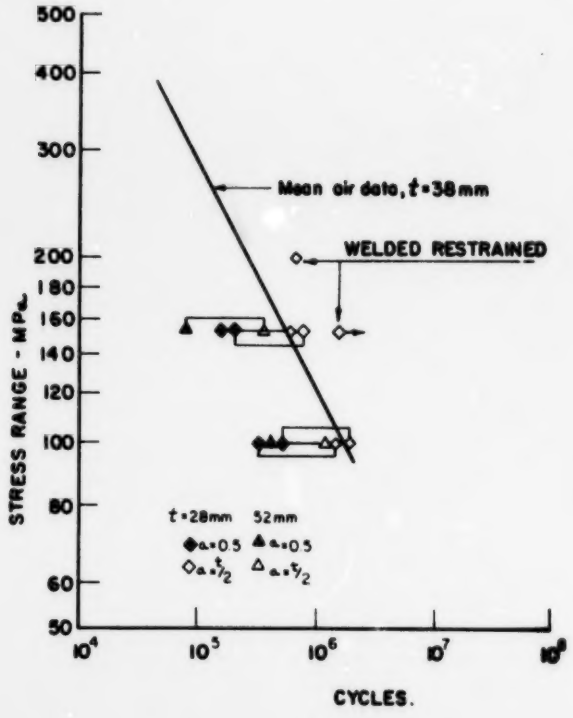

Fig. 7. Total and initiation lives of tested specimens compared with mean total fatigue life curve for 38 mm thick cruciform joints tested at R = 0 and -1, [4].(neg 10502)

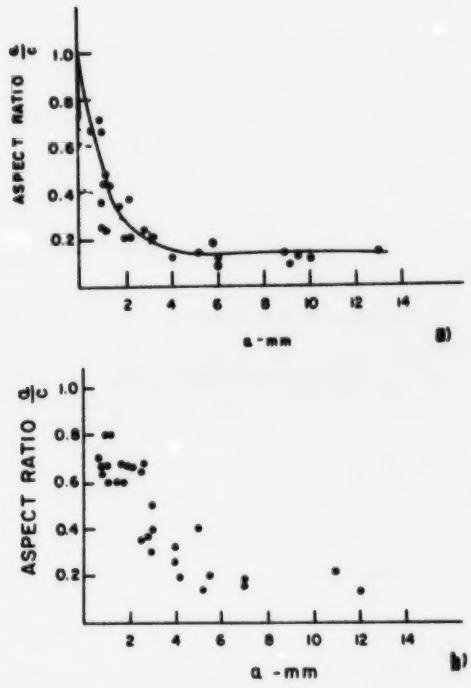

Fig. 8. Variation of crack shape (aspect ratio) with crack depth. (neg 10505)
a) joints 28 mm thick (sepc. No. 3-6) with unimproved weld profile;
b) joints 52 mm thick (sepc. No. 1-2) with improved weld profile.

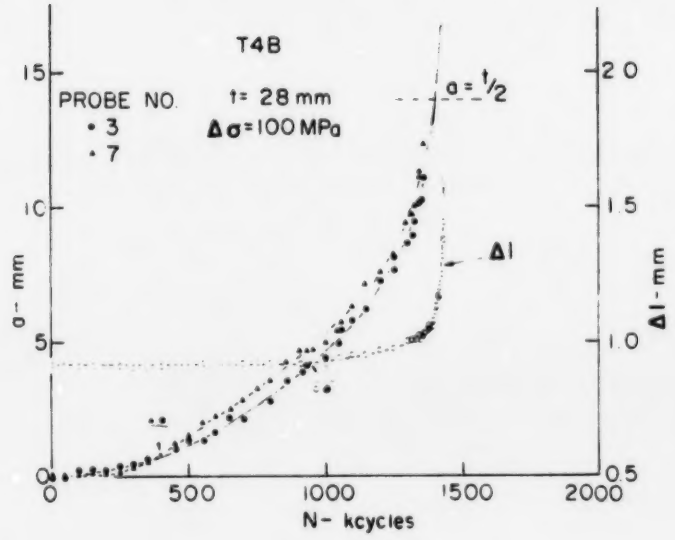

Fig. 9. Variation of crack depth for pro first iniating cracks and displacement range $\Delta\ell$ with number of cycles N. Spec No. 3, t = 28 mm. (neg 10496)

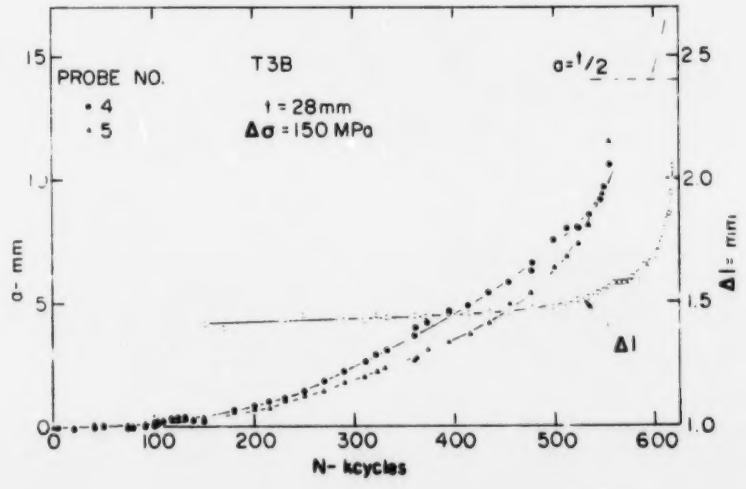

Fig. 10. Same as Fig. 9. Spec. No. 4, t = 28 mm. (neg 10494)

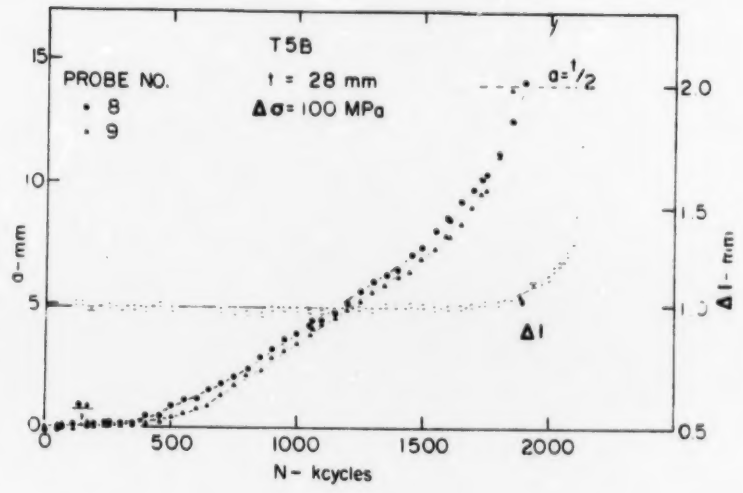

Fig. 11. Same as in Fig. 9. Spec. No. 5, t = 28 mm. (neg 10495)

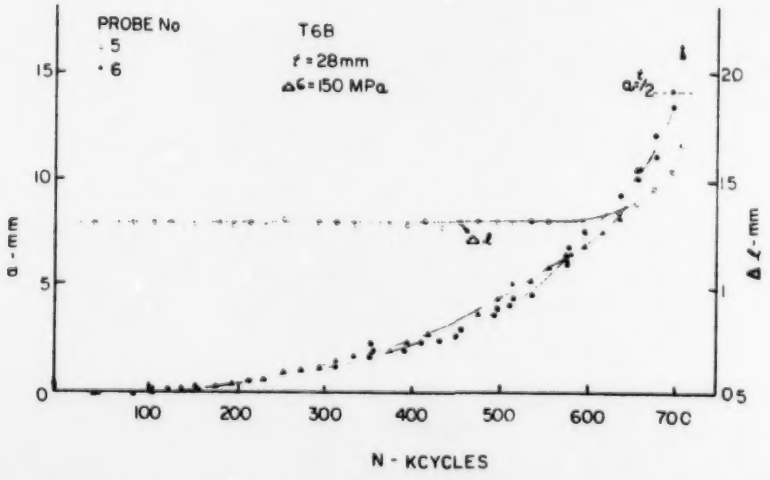

Fig. 12. Same as in Fig. 9. Spec. No. 6 t = 28 mm. (neg 10503)

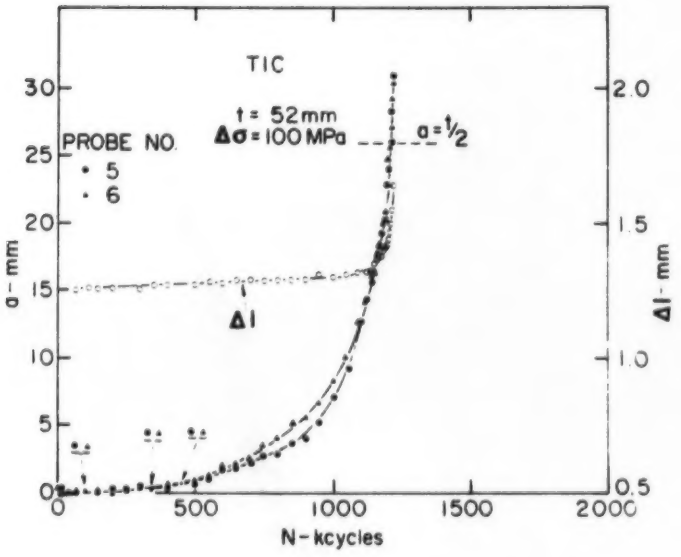

Fig. 13. Same as in Fig. 9. Spec. No. 1, t = 52 mm. (neg 10497)

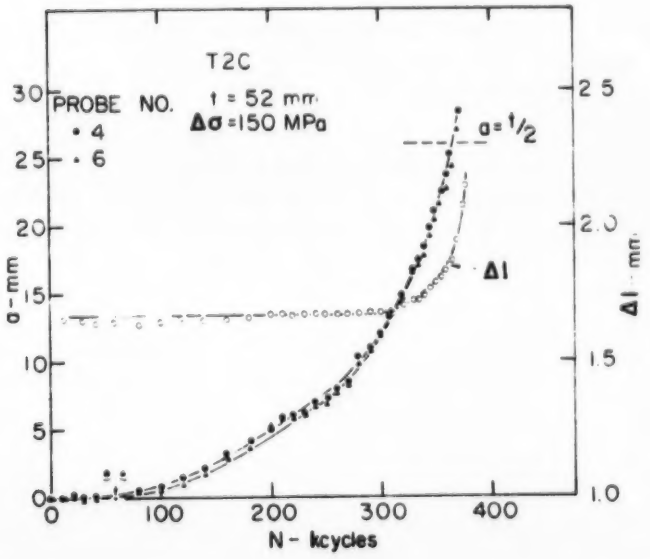

Fig. 14. Same as in Fig. 9. Spec. No. 2, t = 52 mm. (neg 10498)

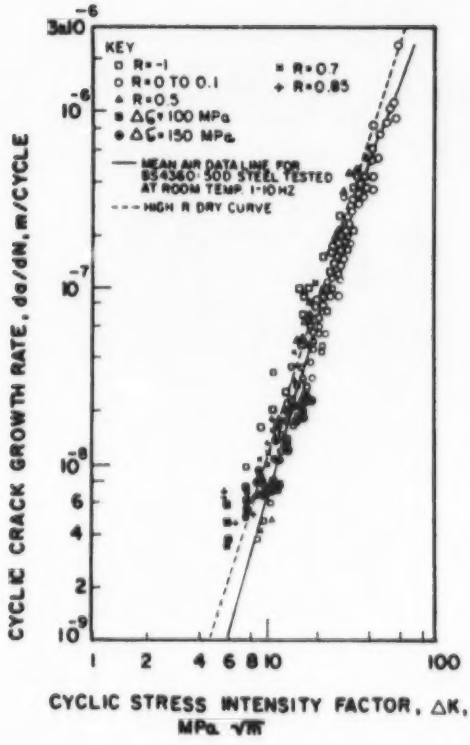

Fig. 15. Fatigue crack growth rates measured on 28 mm thick T-joints compare with fatigue crack growth rates measured on standard specimens with stress ratios R = t to 0.85 [9]. (neg 10499)

POOR

QUALITY

ORIGINAL